Title

Evaluation of the suitability of different calorimetric methods to determine the enthalpy-temperature curve of granular PCM composites

Authors

Javier Mazo*, Mónica Delgado, Conchita Peñalosa, Pablo Dolado, Inés Miranda, Ana Lázaro, José María Marín, Belén Zalba

Aragón Institute for Engineering Research (I3A), Thermal Engineering and Energy Systems Group, University of Zaragoza

Agustín Betancourt Building, C/María de Luna 3, 50018 Zaragoza, Spain

Phone: (+34) 876 555 584

* Corresponding Author, jmazo@unizar.es

Abstract

The present research has analysed the complementarity of different measuring methodologies when characterizing the phase changing behaviour of a granular PCM composite (GPCC) through a comparison of their results. Specifically, the enthalpy variation of the GR31 product manufactured by Rubitherm has been measured by using: 1) An energy balance calculation of an air stream flowing through a GPCC packed bed; 2) Differential Scanning Calorimetry; 3) the T-history method. The main purpose of this study was to evaluate the suitability of these methods for the enthalpy-temperature curve determination of GPCC. The energy balance setup gave an accurate measurement of the enthalpy variation within a sufficiently high temperature interval. Obtaining a representative sample was not a problem using this method, in contrast to the DSC which requires a greater number of tests to obtain an average value representative of the packed bed. However, the energy balance method does not enable the direct determination of the enthalpy-temperature curve. The T-history methodology allows the enthalpy to be determined based on temperature while the representativeness problem of the DSC is avoided due to the higher sample volume. Nevertheless, the sample must be altered, crushed and subsequently compacted to reduce the effects of the thermal resistances provoked by the void spaces being filled by air. This comparison has shown that there is no single valid methodology for characterizing the phase changing behaviour of PCM granules.

Keywords

Thermal Energy Storage; PCM granules; Packed bed; DSC; T-history

Nomenclature

A	Surface	$[m^2]$
a_b	Compactness of the packed bed	$[m^{-1}]$

47	Bi	Biot number $Bi=h \cdot r/(2 \cdot \lambda)$ [-]
48	c	Specific heat capacity [kJ/(kg·K)]
49	C	Constant
50	D	Diameter [m]
51	E	Energy [kJ]
52	e	Thickness [m]
53	f	Liquid mass fraction [-]
54	h	Heat transfer coefficient [W/(m^2·K)], Specific enthalpy [kJ/kg]
55	H	Enthalpy [kJ]
56	L	Thermal losses [kJ]
57	L_b	Length of the packed bed [m]
58	$\dot{m}$	Mass flow [kg/s]
59	m	Mass [kg]
60	Nu	Nusselt number [-]
61	Ra	Rayleigh number [-]
62	T	Temperature [°C]
63	T_m	Phase change temperature [°C]
64	t	Time [s]
65	$\dot{V}$	Air volumetric flow rate [l/min]

66	x	Position [m]

67 **Abbreviations**

68	EB	Relative to the energy balance setup
69	DSC	Differential Scanning Calorimeter
70	GPCC	Granular PCM composites
71	PCM	Phase Change Materials

72 **Subscripts**

73	∞	Ambient conditions, final stationary situation
74	a	Air
75	b	Packed bed
76	c	Relative to convection
77	c,b	Convection in the packed bed
78	eq	Equivalent
79	ext	External
80	i	Inlet
81	int	Internal
82	l	Liquid
83	o	Outlet
84	p	Relative to a particle of the packed bed

r-c	Combined radiation and convection
s	Solid
sur	Surface
t	Tube

Greek symbols

δ	Deviation
Δ	Increase
ε	Emissivity [-]
μ	Mean value
ρ	Density [kg/m^3]
σ	Standard deviation

1. Introduction

Granular PCM composites (GPCC) are of considerable interest for thermal energy storage systems due to the possibility of direct contact between the heat transfer fluid and the GPCC, which can also lead to better heat transfer rates while taking advantage of small particle diameters. These composites provide a flexible solution that can be used in several applications. On the one hand, they can be integrated with air heat exchangers. Several configurations have been experimentally analyzed. Packed bed air heat exchangers have been studied by Nagano et al. [1] and Rady [2,3] whereas various fluidized bed configurations have been exhaustively tested by Izquierdo-Barrientos et al. [4] and Izquierdo-Barrientos et al. [5]. For building applications, Nagano et al. [6] proposed and tested at small scale a floor supply air conditioning system where a packed bed was installed in order to

shift cooling energy consumption to the night period. On the other hand, PCM granules can be integrated into building composite materials. Hawes [7] proposed this technique for incorporating PCM into concrete. Since then, a substantial number of works has been published on the preparation and analysis of light weight concretes [8-10] and mortars [11-13] with PCM contained in porous particles.

Characterization of the phase changing behaviour of granular materials is an important issue for the design and optimization of latent thermal energy storage systems. However, PCM embedded into granular porous solids may present difficulties when measuring enthalpy-temperature curves. Differential scanning calorimeter (DSC) is a popular method of determining phase change enthalpy and phase change temperature. In general, the representativeness of the sample has to be ensured, but this can be compromised in DSC measurements as the sample frequently has a similar magnitude as the GPCC granules. Since the PCM absorption is expected to be unequal between different granules, a specific analysis of the heterogeneity of the composite material should be made before presenting a result.

The DSC technique has been widely used for the characterization of GPCC. For instance, it was used in the works of Kheramad et al. [14] and Sharifi and Sakulich [15], dealing with the preparation of GPCC for incorporating PCM into lightweight aggregates that can be integrated into construction materials, in order to determine the thermal energy storage capacity. Izquierdo-Barrientos et al. [16] evaluated the stability through melting and solidifying cycles of the storage capacity of these particles for their application in a fluidized bed heat exchanger. Rady [17] and Kheradmand et al. [14] showed the significant influence of the temperature variation rate used in their experiments on the phase change temperature interval determination, while its effect on the associated enthalpy variation was of secondary importance. Taking this fact into account, Rady [17] and Rady and Arquis [18] proposed a method, based on the adjustment of a thermal model representing the DSC device, in order to correct the error associated with a non-thermal equilibrium temperature variation rate. However, a wide range

of heating and cooling rates (0.5-10K/min) has been used in the evaluation of the storage capacity of GPCC. Although the suitability of this relevant testing parameter depends on additional aspects such as the thermal conductivity of the porous matrix or the sample preparation, the effect of this heating and cooling rate is not frequently evaluated when the experimental data obtained from this technique are presented.

Rady [17] recognized that special attention has to be paid to the sample preparation when measuring GPCC in order to ensure the representativeness of DSC samples. However, little detailed information is usually provided about this feature. Some exceptions include Zhang et al. [19], Zhang et al. [20], Li et al. [21] and Li et al. [22] who specified that crushed samples were used. Additionally, Zhang et al. [19] and Zhang et al. [20] investigated the influence of this modification of the composite structure on the phase transition temperature. Concerning the number of samples, Izquierdo-Barrientos et al. [16] used five sets of two samples in order to analyse the storage capacity stability through melting and solidifying cycles.

In contrast to DSC, by using the T-history method [23], the sample representativeness problem is solved. The sample volume is at least one order of magnitude higher than the particle size. However, it is difficult to verify if the theoretical limit imposed on the Biot number of the PCM is satisfied, since the resulting thermal conductivity of the sample contained in the sample is not frequently known. Additionally, as has been numerically analyzed in Mazo et al. [24], measuring solids with the highest Biot number values permitted by this methodology (Bi=0.1) can lead to significant deviations in the enthalpy-temperature curve.

Compared to DSC, fewer works dealing with PCM granules and the T-history methodology have been found in literature. Rady et al. [25] and Rady and Arquis [18] performed cooling T-history tests on GR27 and GR42 samples (Rubitherm [26]). They proposed a modification to the original method [30] in order to identify the beginning and end of the solidifying process. Additionally, they applied

155 the method proposed by Marín et al. [27] in order to integrate empirical data into the enthalpy-
156 temperature curve.

157 On the other hand, with an air heat balance installation, whose methodology is based on the same
158 physical principle as that of the energy balance experimental installations developed by Zalba et al.
159 [28] or Günther et al. [29], the enthalpy variation of PCM granules in a packed bed can be quantified.
160 Although this proposed methodology cannot evaluate the enthalpy-temperature curve, it can provide
161 a direct and accurate measurement of the thermal energy variation of a GPCC packed bed between
162 the final and initial temperatures of the experimental test.

163 Finally, it has to be taken into account that the changes in the PCM supporting structure associated to
164 sample preparation (e.g. when crushed samples are used) can modify the phase change behaviour of
165 the composite material. In fact, the interaction between the PCM and the supporting porous structure
166 can lead to certain changes in phase change temperature and enthalpy [30]. Concerning its influence
167 on melting and solidifying temperature, Zhang et al. [20] identified two main effects. On the one
168 hand, the confinement inside a porous structure induces pressure variations in the PCM which are
169 associated with the volume expansion during the phase change process that modifies the melting
170 temperature. This effect can be evaluated by the Clapeyron equation. As a result of this phenomenon,
171 the confinement (or the reduction of mean pore size) produces an increase in the melting temperature
172 for most PCM ($\rho_s > \rho_l$). On the other hand, the interaction between the PCM and the inside porous
173 surface modifies the phase change temperature. This effect can be explained with the Gibbs-Thomson
174 equation. For attractive interaction between the pore surface and the liquid, the melting temperature
175 increases, whereas it decreases if the interaction is weak or repulsive. Zhang et al. [20] found that
176 capric acid showed a remarkable increase in the melting temperature when confined in pores, which
177 was explained in terms of the confinement effect and the attractive interaction of the PCM. However,
178 they did not observe any significant variation in phase change temperature in paraffin. The authors
179 explained that in the latter cases, both phenomena produced an opposite effect. Furthermore, Zhang

et al. [19] observed that the phase change temperature range was affected by the porous material and also by the PCM volume fraction in composites. Zhang et al. [31] also studied different porous media as the matrix for organic PCMs. They observed that there was a wider phase change temperature range when relatively pure organic PCMs were confined. In the case of phase change enthalpy, a reduction of its value –if it is compared to the bulk PCM material– can generally be expected as a result of the confinement [30]. Nevertheless, the intensity of this reduction depends both on the PCM and on the porous structure. Fu et al. [32] investigated the effect of the incorporation to a SiO_2 matrix of different organic materials. They observed a slight reduction of about 5% in the phase change enthalpy of paraffin composites.

The present study aims to evaluate the suitability of these three measuring methodologies –DSC , T-history and air energy balance– for the enthalpy-temperature curve determination of GPCC. A similar approach was used by Günther et al. [33] for the thermal characterization of pure PCM and PCM macrocapsules. In their work, the results from DSC –obtained with both the dynamic and isothermal step modes–, T-history and an air flow energy balance installation were compared. They discussed the suitability of DSC methods and found good agreement between the macrocapsule experimentation in the air balance set up and the T-history results for a PCM with a significant sub-cooling phenomenon. In the present work, the experimental results of these methods for the thermal characterization of a granular material have been analyzed and compared.

2. Materials

The product GR31, supplied by the manufacturer Rubitherm [26], has been characterized. These granules have a particle size between the range of 1-3 mm, where paraffin is absorbed, representing a mass fraction of approximately 35%, inside a porous mineral structure which contains diatom (according to patent EP1628110A1, 2006 [34]). Figure 1 shows a picture of the analysed commercial

GPCC. According to manufacturer information, the composite undergoes an enthalpy variation of 60kJ/kg (±7.5%) within the temperature range from 20 to 35ºC [26].

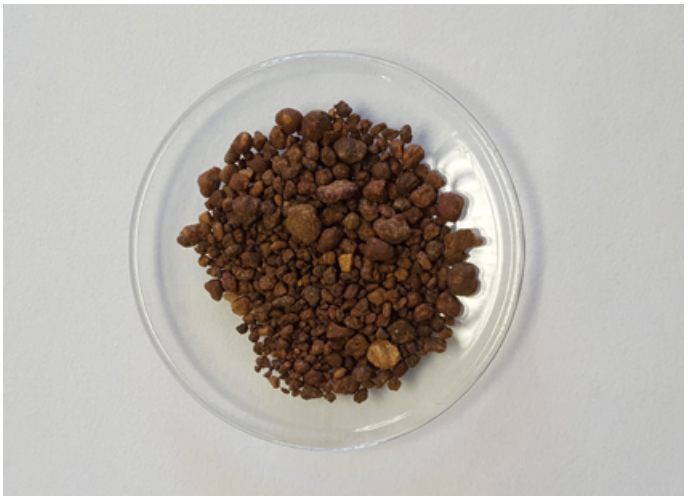

Figure 1. Image of the analysed GPCC (GR31 [26]).

3. DSC measurements

3.1 Methodology adopted

The present work adopts the methodology for characterizing phase change materials with a DSC proposed by Lázaro et al. [35] after a set of Round Robin Tests. Firstly, heating and cooling rates were applied to the PCM, starting from fast rates (10 K/min) and slowing down by halving the previous rate. When the changes in peak temperature between two consecutive tests were lower than 0.2 K, thermal equilibrium in the sample and crucible could be assumed. The highest heating rate once this condition of thermal equilibrium was achieved has been taken as the equilibrium rate. The calibration was performed by using seven different standards (mercury, water, gallium, indium, tin, bismuth and cesium chloride) at the equilibrium heating rate, as well as the baseline measurement (empty crucible). Once these measurements were accomplished, the same or a lower sample mass was measured at the equilibrium rate to ensure thermal equilibrium. Three samples and three cycles were applied and the baseline subtracted from the results obtained.

As previously mentioned, the characterization of GPCC using DSC requires special care to ensure that the measured sample is representative of the bulk material used in practical solutions. Due to the heterogeneity of the sample and to the crucible volume, achieving a representative sample can be a problem. Also the morphological structure of the granules can have an influence on the heat transfer process depending on the contact resistance with the crucible. In order to analyse this representativeness problem, two different approaches have been followed with regard to the sample preparation. On the one hand, granules with a flat surface were taken as samples to be measured, placing the flat face on the crucible base to avoid an elevated thermal contact resistance. On the other hand, PCM granules were crushed and subsequently compacted in the aluminium crucible, the quantity being equivalent to that of one whole granule. Three samples of each preparation methodology were tested.

The equilibrium condition was reached between the heating rate of 0.125 and 0.0625 K/min for both types of sample (crushed and granule), having a sample mass of 27.93 mg for the crushed sample and 28.23 mg for the individual PCM granules. As a result of these equilibrium tests, measurements have been executed at 0.125 K/min. Figure 2 shows the results for the crushed sample and figure 3 for the granule sample.

Additionally, complementary measurements of the specific heat capacity have been made following the procedure defined in [36], using sapphire as the reference material. Two samples of, respectively, granulated and crushed GPCC were tested at a speed of 1K/min. Finally, the methodology proposed in the *Guide for the expression of the uncertainty in measurement* [37] has been used to analyse the uncertainty propagation through DSC results. Rudtsch [38] and Wilthan [39] applied this procedure to the evaluation of the resulting uncertainty interval of specific heat capacity and temperature measurements, whereas Sarge et al. [40] presented an example where that range associated with phase change enthalpy was calculated. As in these previous works, repeatability of DSC signals and temperature measurements have been the principal contributions to the overall uncertainty.

3.2 DSC results

In figure 2 a different result can be observed for the first crushed sample between the first heating and the two following ones. This effect is principally associated with a deviation in the measurement of specific capacity. It has to be noted that at the thermal equilibrium speed the intensity of the signal corresponding to the sensible contribution to the overall thermal energy variation of the sample is low. A similar behaviour was observed for the other two samples tested. The second and third heating processes for all the samples have similar results. The enthalpy variation measured in the third test of each crushed sample is presented in Table 1, showing maximum differences of around 4%. This can also be observed in figure 2 (right). On the other hand, a possible leak of the paraffin soaked by the silica supporting material could been observed with the naked eye. After the bulk material was cycled, the sample turned darker due to the paraffin leak.

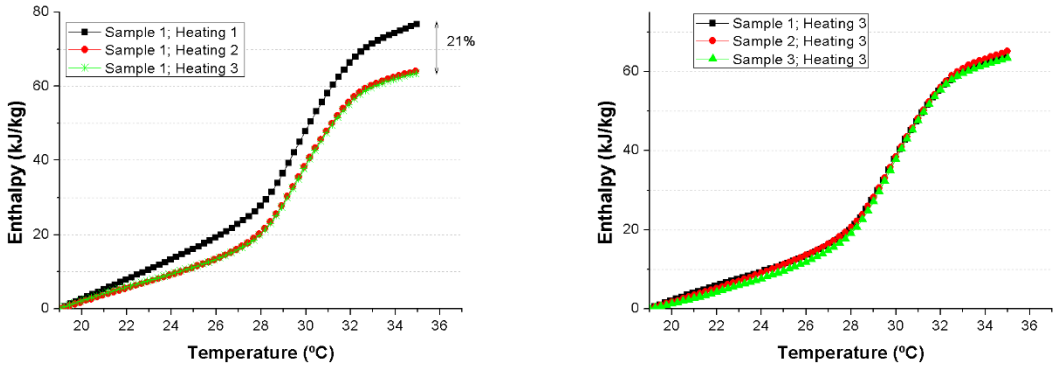

Figure 2. DSC results when GR31 is crushed. Left: Enthalpy-Temperature curve for sample 1 for 3 consecutive heating tests. Right: Enthalpy-Temperature curve for samples 1, 2 and 3 during the third heating.

The same behaviour is observed in figure 3 in the case of testing with a granule of GR31 with a flat surface set on the crucible base. The second and the third heating gave rise to a different result than that of the first heating. However, in contrast to the crushed sample, it is observed that the results vary depending on the granule (figure 3 left), so the samples do not seem to be representative. Differences

up to 20% were measured between the analysed samples (table 1). More samples would be necessary to reduce the dispersion of the results of this measurement of the enthalpy variation of the granulated material. In addition, due to the possible different absorption of PCM in each granule, a thermal equilibrium test should be run for each sample to be measured, instead of measuring just one sample and then applying the resulting equilibrium rate to the rest of the samples.

The significant reduction in the variability of the results using crushed samples can be associated with a lower effect of the heterogeneity of the composite material on DSC results. Therefore, taking into account this statistical indicator, measuring crushed GR31 samples can be recommended. However, it has to be taken into account that the crushing process can modify the confinement of PCM.

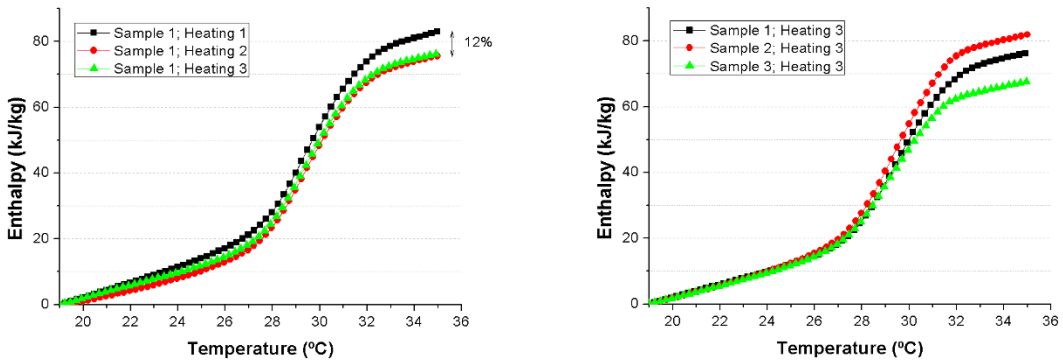

Figure 3. DSC results for GR31 granules. Left: Enthalpy-Temperature curve for sample 1 for 3 consecutive heating tests. Right: Enthalpy-Temperature curve for samples 1, 2 and 3 during the third heating.

In figure 4, the third heating of each crushed and granule sample has been compared. It is observed that for the crushed samples, similar results in terms of phase change enthalpy and phase change temperature are obtained, as previously mentioned. In the case of the granule samples, deviations in terms of phase change enthalpy are observed, probably due to the different mass fraction of paraffin absorbed by the silica matrix.

Concerning the phase change temperature, an additional quantification has been made. The main purpose of this analysis is to compare the DSC results to those obtained from T-history method. It has to be noted that in the latter, due to relevant effect of the noise and the precision of temperature measurements, the evaluation of the specific heat capacity at a given temperature level has a significant uncertainty range [41]. Consequently, the determination of peak temperature with this method is uncertain. The proposed additional analysis is based on the evaluation of the evolution of the liquid mass fraction curve $f(T)$. This dimensionless function is defined by the following model describing the variation of enthalpy with temperature (Eq. 1). Palomo del Barrio and Dauvergne [42] used this approach in order to describe the enthalpy-temperature curve of a PCM composite material which was determined by means of an inverse method.

$$\frac{dh}{dT} = c_{eq}(T) = c_s + (c_l - c_s)\cdot f + h_m \cdot \frac{df}{dT} \quad (1)$$

Where c_s and c_l are the specific heat capacity values corresponding to the solid and liquid states are measured at 22°C and 35°C respectively. Therefore, for a given enthalpy-temperature curve, the temperature dependence of the liquid fraction ($f(T)$) can be calculated by solving the previous first order differential equation (Eq. 1, imposing the initial condition $f(T_s) = 0$) thus resulting in the following expression (Eq. 2).

$$f(T) = \frac{h(T)}{h_m} - \frac{c_s}{c_l - c_s}\cdot\left[1 - e^{\frac{c_l - c_s}{h_m}\cdot(T - T_l)}\right] - \frac{c_l - c_s}{{h_m}^2}\cdot e^{-\frac{c_l - c_s}{h_m}\cdot T}\cdot\int_{T_l}^{T} e^{\frac{c_l - c_s}{h_m}\cdot\tau}\cdot h(\tau)\cdot d\tau \quad (2)$$

The definite integral in equation 2 has been numerically calculated at each temperature level by means of the trapezoidal rule. Additionally, the parameter h_m, which is the one that verifies the condition $f(T_l) = 1$, has been calculated using an iterative scheme. Finally, an average phase change temperature ($\overline{T}_m$) is quantified from experimental results with the following equation (Eq. 3).

$$\overline{T}_m = \frac{\int_{0.05}^{0.95} T \cdot df}{0.9} \qquad (3)$$

The measured values of peak temperatures (T_p) and average phase change temperature ($\overline{T}_m$) are presented in table 1, whereas the temperature evolutions of equivalent heat capacity ($c_{eq}(T) = \frac{dh}{dT}$) and the liquid fraction are shown in figure 5. It is interesting to highlight the difference in the melting temperature (approximately 0.5K, see table 1) between the crushed and the granule sample. In principle, this could be explained by a lack of thermal equilibrium, since this thermal equilibrium test was done with one only sample and the resulting heating rate directly applied to the other three samples which could be different. However, this would lead to a shift toward higher temperatures instead of lower temperatures. The crushed sample preparation could have led to this variation in the phase change temperature. Conversely, due to the high dispersion of the results of the granule samples, the effect of the modification of the porous structure on the phase change enthalpy cannot be analysed. A specific study should be carried out in order to evaluate these effects in the analysed composite material, which is beyond the scope of this work. Nevertheless, when measuring the enthalpy-temperature curve of these composites, it is recommendable to verify that the sample preparation does not significantly modify the phase change process.

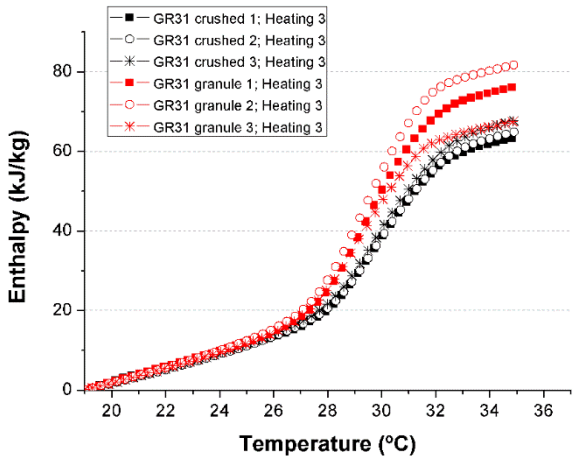

Figure 4. Comparison of the DSC curves for the third heating for all the samples, in crushed form and in granule form.

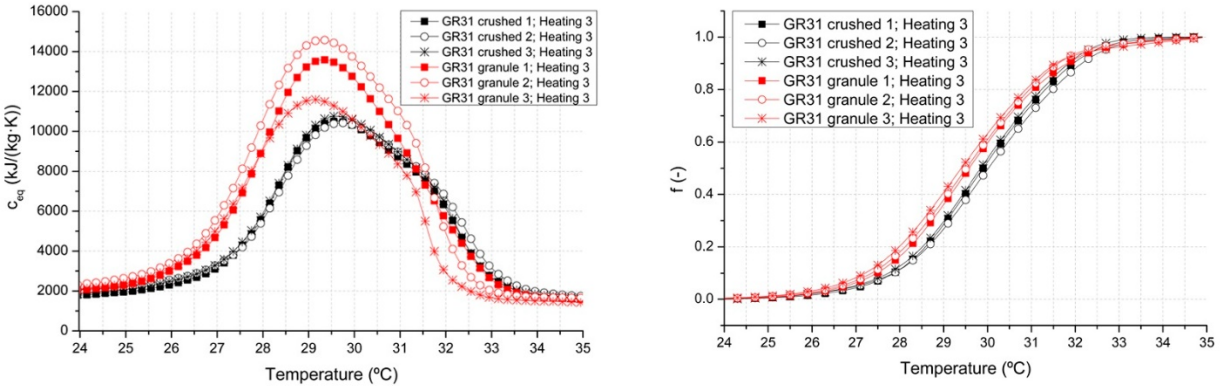

Figure 5. Analysis of the measured phase change temperature interval. Left: temperature dependence of equivalent specific heat capacity. Right: temperature dependence of the liquid fraction dimensionless parameter (f, Eq. 1).

	Crushed sample				**Granule sample**			
	Sample 1	Sample 2	Sample 3	μ (σ)	Sample 1	Sample 2	Sample 3	μ (σ)
Mass (mg)	12.12	20.69	21.53	-	15.6	23.41	21.91	-
T_p [°C]	29.6±0.3	29.7±0.3	29.6±0.3	29.6±0.3 (0.06)	29.3±0.3	29.3±0.3	29.1±0.3	29.3±0.3 (0.13)
$\overline{T}_m$ [°C]	29.9±0.3	29.9±0.3	29.9±0.3	29.9±0.3 (0.06)	29.5±0.3	29.4±0.3	29.2±0.3	29.4±0.3 (0.13)
Enthalpy variation (25-35°C) [kJ/kg]	52.4±3.1	53.9±3.2	54.4±3.3	54±2 (1.0)	64.3±3.9	69.5±4.2	55.9±3.4	63.6±17.9 (6.9)
	Sample 1'	Sample 2'		μ (σ)	Sample 1'	Sample 2'		μ (σ)
Specific heat (20-22°C) [kJ/(kg·K)]	1.59±0.08	1.58±0.08		1.60±0.05 (0.01)	1.86±0.09	1.71±0.09		1.8±0.3 (0.11)
Specific heat (35-40°C) [kJ/(kg·K)]	1.37±0.10	1.38±0.10		1.37±0.07 (0.01)	1.55±0.11	1.42±0.10		1.5±0.2 (0.09)

Table 1. Mass, melting temperature and enthalpy variation (25-35°C) according to the DSC.

4. T-history measurements

The material analyzed in the present study, GR31, has been measured in a T-history installation, whose technical details are described in the Ph.D. dissertation by Lazaro [43]. The method proposed by Marín et al. [27] has been used in order to obtain the enthalpy-temperature curve. Due to the limitations of the chamber for high temperatures, only the results of cooling tests are presented in this work.

Samples were prepared by crushing the GR31 granules in a lab mortar. The material was subsequently compacted in the sample holder of the T-history set-up. Special attention must be paid in this compacting process to reduce the effects related to thermal resistances resulting from the intergranular space filled by air, to avoid radial thermal gradients inside the sample. These thermal gradients could lead to significant deviations in the enthalpy-temperature curve determination by the T-history methodology [44, 45]. Furthermore, when testing solid PCM, this effect is expected to be more significant due to the fact that heat transfer takes place only by conduction.

According to the results of Mazo et al. [24], who theoretically analyzed the conduction transfer process inside T-history samples, when the temperature is measured in the centreline, phase change enthalpy can be overestimated in 10% if the tests are carried out at limit Biot numbers (Bi ≈0.1). On the other hand, when the temperature is measured at the surface of the sample holder, the deviation in phase change enthalpy is negligible and is not expected to depend on the thermal properties of the PCM sample. Therefore, in these experiments this last configuration was selected for temperature measurements.

Type T thermocouples were used for measuring the temperature at the sample surfaces. The uncertainty of the temperature measurement (±0.5°C) has been considered in the presentation of the results. For this purpose, the methodology proposed by Mazo [41] for evaluating the uncertainty propagation across the enthalpy-temperature curve integration process [27] has been used. In figure 6 the temperature evolution during the third experiment is shown whereas the results of three T-history tests are gathered in table 2. The enthalpy-temperature curve obtained is presented in section

6, where the outcomes of the different measuring methods are compared (fig. 10). The results show a reasonable repeatability which is lower than the calculated measurement uncertainty range.

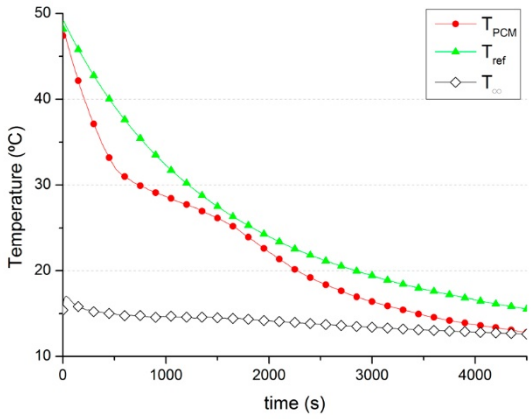

Figure 6. Registered time evolutions during T-history test 3 (heat capacity of T-history components: $C_{ref} = m_{ref} \cdot c_{ref} = 154$J/K, $C_t = m_t \cdot c_t = 51$J/K).

Test	m_{PCM} [g]	$c_{p,s}$ [J/(kg·K)]	$c_{p,l}$ [J/(kg·K)]	Δh [kJ/(kg·K)] (25-35°C)	T_m [°C]
T1	34.81	1.3 ± 0.4	1.6 ± 0.4	52 ± 3	29 ± 0.5
T2	34.81	1.4 ± 0.4	1.6 ± 0.4	51 ± 3	29 ± 0.5
T3	34.81	1.3 ± 0.4	1.5 ± 0.4	53 ± 3	29 ± 0.5
Repeatability (σ)	-	0.03	0.06	1.00	0.10

Table 2. Summary of the results of T-history cooling tests.

5. Air energy balance installation

The experimental installation previously developed by Dolado et al. [46] has been used for these measurements as it allows the measurement of the enthalpy variation of a packed bed of granular PCM. In figure 7 a sketch of the experimental set up is provided. The air flow temperature is measured at the air inlet and outlet sections. Additionally, the surface temperature of the glass container is measured at three points. Type T thermocouples are used for these measurements. The air volumetric

flow is measured by a thermal mass flow controller (Bronkhorst, EL-FLOW [47]). The uncertainty associated with each measurement is presented in table 3 and discussed in section 5.1. The GPCC packed bed is contained inside a glass tube (D_{int}=22 mm, D_{out}=26 mm, e=2 mm).

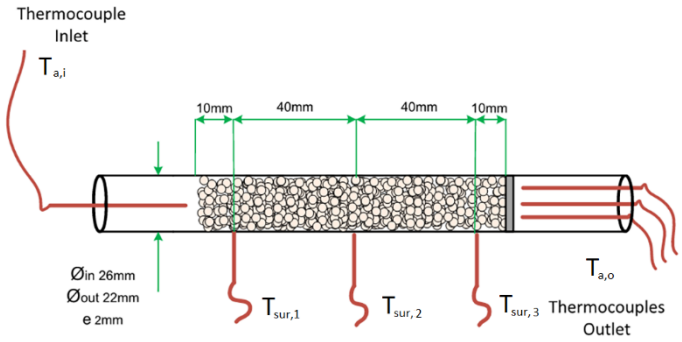

Figure 7. Sketch of the experimental set up.

Equation 4 represents the energy balance equation giving the enthalpy change between the beginning and the end (t_∞) of the experiment. Four main contributions are considered: energy balance to the air flow (ΔH_a), heat losses (L), and the thermal energy variations corresponding to the PCM packed bed (ΔH_{PCM}) and to the tube (ΔH_t). In this energy balance equation, thermal gains and losses due to the axial conduction heat transfer through the tube at the inlet and outlet sections and the time variation of the air flow thermal energy are neglected.

$$m_{PCM}\cdot\Delta h_{PCM} = \int_{t=0}^{t_\infty}\left(T_{a,i} - T_{a,o}\right)\cdot\dot{m}_a\cdot c_{p,a}\cdot dt - \int_{x=0}^{L_b}\left(T_t\big|_{t_\infty} - T_\infty\right)\cdot\frac{m_t}{L_b}\cdot c_{p,t}\cdot dx -$$

$$- \int_{t=0}^{t_\infty}\left(T_\infty - \overline{T}_t\right)\cdot h_{r-c}\cdot A_t\cdot dt = \Delta H_a - \Delta H_t - L \qquad (4)$$

The equivalent radiative and convective thermal coefficient (h_{r-c}) is obtained from the final stationary situation (Eq. 5). Its radiative and convective components have been corrected at each time step of the experiment from the value calculated at the stationary situation. For this purpose, radiation heat exchange has been modelled considering the tube as small object with a grey surface (ε_t=0.9) enclosed in a small cavity [48] (Eq. 6). On the other hand, free convection coefficient has been represented by

an expression of the form $Nu=C\cdot Ra^n$. If the variation of air thermophysical properties during the thermal test is neglected, the free convection heat transfer coefficient can be approximated by the following expression ($h_c \approx C^{'}\cdot\left(\overline{T}_t - T_\infty\right)^n$) (Eq. 6). According to the correlation of Churchill and Chu [49], an exponent of 0.33 for the Raleigh number has been used.

$$h_{c-r}\Big|_{t_\infty} = \frac{\dot{m}_a\cdot c_{p,a}}{A_T}\cdot\frac{\left(T_{a,i} - T_{a,o}\right)\Big|_{t_\infty}}{\left(\overline{T}_t\Big|_{t_\infty} - T_\infty\right)} \quad (5)$$

$$h_{c-r}\Big|_{t_\infty} = \varepsilon_t\cdot\sigma\cdot\left(\overline{T}_t\Big|_{t_\infty}{}^2 + T_\infty{}^2\right)\cdot\left(\overline{T}_t\Big|_{t_\infty} + T_\infty\right) + C'\cdot\left(\overline{T}_t\Big|_{t_\infty} + T_\infty\right)^{0.33} \quad (6)$$

5.1 Uncertainty propagation analysis

The uncertainty propagation of the measurements through the energy balance equation (Eq. 4) has been taken into account in order to select the most favourable conditions (air inlet temperature, length of the packed bed and air volumetric flow rate) in which to carry out these experiments. Equation 7 represents this uncertainty propagation law [37] including the uncertainty of each term contributing to the energy balance equation. The accuracy of the method depends on the relation between the contributions to the energy balance equation. Due to the uncertainty propagation law, one important effect on the overall error is the amplification effect of the factor $\Delta H_a/\Delta H_{PCM}$. Considering this fact, it is more advisable to work at low values of this relation (lower heat losses and thermal inertia of the tube) than to have a very accurate measurement of these secondary terms.

$$\frac{\delta(\Delta H_{PCM})}{\Delta H_{PCM}} = \sqrt{\left(\frac{\Delta H_a}{\Delta H_{PCM}}\right)^2\cdot\left(\frac{\delta(\Delta H_a)}{\Delta H_a}\right)^2 + \left(\frac{\Delta H_t}{\Delta H_{PCM}}\right)^2\cdot\left(\frac{\delta(\Delta H_t)}{\Delta H_t}\right)^2 + \left(\frac{L}{\Delta H_{PCM}}\right)^2\cdot\left(\frac{\delta(L)}{L}\right)^2} =$$

$$= \sqrt{\left(1 + \frac{\Delta H_t}{\Delta H_{PCM}} + \frac{L}{\Delta H_{PCM}}\right)^2\cdot\left(\frac{\delta(\Delta H_a)}{\Delta H_a}\right)^2 + \left(\frac{\Delta H_t}{\Delta H_{PCM}}\right)^2\cdot\left(\frac{\delta(\Delta H_t)}{\Delta H_t}\right)^2 + \left(\frac{L}{\Delta H_{PCM}}\right)^2\cdot\left(\frac{\delta(L)}{L}\right)^2} \quad (7)$$

The influence of the controllable experimental conditions (air inlet temperature, length of the packed bed and volumetric air flow) in this uncertainty propagation is not simple a priori, and some opposing

effects can be expected. For example, if a high air inlet temperature is selected, although the relative error in the energy balance estimation to the air flow (ΔH_a) decreases (lower ratio $\delta T/\Delta T_{a,i-o}$), heat losses and energy variation of the glass tube ratios ($\Delta H_t/\Delta H_{PCM}$, $L/\Delta H_a$) are expected to increase, thus amplifying this error. Consequently, a preliminary numerical analysis has been made in order to obtain a prediction of these contributions to the energy balance equation at different testing conditions. In this way, an estimation of the resulting measurement uncertainty interval in a variety of situations can be calculated. In section 5.1.1 the numerical model is briefly described, whereas the parametric analysis that has been carried out with the purpose of determining a range of favourable testing conditions is presented in section 5.1.2.

Table 3 gathers the information about the sensors used in the experimental setup and their associated uncertainty. The uncertainty of each contribution to the energy balance equation (Eq. 4) has been calculated using the uncertainty propagation law with equations 8, 9 and 10. Their values will be shown in section 5.4.

$$\frac{\delta EB_a}{EB_a} = \sqrt{\left(\frac{\delta \dot{m}_a}{\dot{m}_a}\right)^2 + \left(\frac{\delta(\Delta T_a)}{\overline{\Delta T_a}}\right)^2}\ ; \qquad \frac{\delta H_t}{H_t} = \sqrt{\left(\frac{\delta c_t}{c_{p,t}}\right)^2 + \left(\frac{\delta(\Delta T_{sur,\infty})}{\Delta T_{sur,\infty}|_{t_\infty}}\right)^2} \qquad (8\text{-}9)$$

$$\frac{\delta L}{L} = \sqrt{\left(\frac{\delta h_{c-r}}{h_{c-r}}\right)^2 + \left(\frac{\delta(\Delta T_{sur,\infty})}{\overline{\Delta T}_{sur,\infty}}\right)^2} = \sqrt{\left(\frac{\delta \dot{m}_a}{\dot{m}_a}\right)^2 + \left(\frac{\delta(\Delta T_a)}{\Delta T_a|_{t_\infty}}\right)^2 + \left(\frac{\delta(\Delta T_{sur,\infty})}{\overline{\Delta T}_{sur,\infty}}\right)^2} \qquad (10)$$

Magnitude	Sensor	Uncertainty
Air temperature	Thermocouple type T	±0.5°C
Surface temperature	Thermocouple type T	±0.5°C
Volumetric flow rate	Flow controller	±0.6%

Table 3. Uncertainty of the magnitudes measured.

5.1.1 Numerical model

The numerical model which has been developed in order to simulate the heat transfer inside the PCM packed bed is briefly described in this section. The model is based on the following assumptions: uniform temperature inside the PCM granules; uniform temperature across the packed bed section and uniform air flow; heat transfer between the granules and the inside surface of the tube is neglected; time variation of the thermal energy of the air is not considered; and, finally, the tube containing the packed bed is considered as a lumped heat capacity system in radial direction where axial heat conduction inside the tube has been neglected. According to these simplifications, the problem can be represented by the following equations (eq. 11-12), corresponding, respectively, to the energy balance –formulated in its differential form– of the air stream (eq. 11), packed bed particles (eq. 12) and the wall of the tube (eq. 13).

$$\dot{m}_a \cdot c_{p,a} \cdot \frac{\partial T_a}{\partial x} = \frac{\pi \cdot D_b^2}{4} \cdot a_b \cdot h_{c,b} \cdot (T_b - T_a) + \pi \cdot D_b \cdot h_{c,b} \cdot (T_t - T_a) \quad (11)$$

$$6 \cdot h_{c,b} \cdot (T_a - T_b) = D_p \cdot \rho_p \cdot \frac{\partial h_{PCM}}{\partial t} \quad (12)$$

$$(D_b + e) \cdot h_{r-c} \cdot (T_\infty - T_t) + D_b \cdot h_{c,b} \cdot (T_a - T_t) = \frac{(D_b + e)^2 - D_b^2}{4} \cdot \frac{m_t}{L_b} \cdot c_t \cdot \frac{\partial T_t}{\partial t} \quad (13)$$

It should be noted that the main assumptions of the model (one-dimensional analysis, uniform temperature inside PCM granules) are identical to those adopted by Rady [2, 3], Izquierdo-Barrientos [50] and Izquierdo-Barrientos et al. [51]. The prediction of these models has been demonstrated to be accurate enough for the purpose of this work. For the external convective component of the equivalent heat transfer coefficient (h_{r-c}), the correlation from Churchill and Chu [49] has been used, whereas that formulated by Wakao [52] has been utilized for calculating the heat exchange coefficient inside the packed bed ($h_{c,b}$).

An enthalpy method has been used in order to handle the phase change. A fully implicit method has been utilized for time discretization and a central difference scheme has been chosen for the spatial

discretization since, due to the high contact surface, the Peclet number associated to the numerical scheme is 0.6 [53].

5.1.2 Determination of temperature levels and lengths for the packed bed

The previously described numerical model has been used to evaluate the influence of the experimental conditions on the uncertainty propagation of sensor errors during the measurement of the enthalpy variation of the PCM packed bed. The effect of the length of the tube (L_b [mm]), the air inlet temperature ($T_{a,i}$ [°C]) and the air flow (q [l/min]) has been analyzed. The objective is to determine an acceptable range for these conditions where an uncertainty of ±5% is ensured.

In figure 8, the influence of the previously mentioned experimental conditions on the uncertainty of the results is plotted ($\delta h_{PCM}/\Delta h_{PCM}$ [%]). Looking at the effect of the inlet temperature (fig. 8 (a)), it can be seen that the error decreases when the air inlet temperature rises in the temperature range analyzed. In this case, the most important effect on the uncertainty propagation through the energy balance equation is the temperature difference between the air inlet and outlet. Additionally, the influence of the air volumetric flow rate is negligible for this combination of uncertainties of the measured variables. According to these results, the inlet temperature should be selected above 50°C. Concerning the packed bed length (fig. 8 (c, d)), the main influence on the overall uncertainty is the increase in the ratio between heat losses and the enthalpy variation of the PCM ($L/\Delta H_{PCM}$). According to this, packed bed lengths from 40 to 100 mm can be chosen, since they produce an acceptable error in the solution (±5%, fig. 8 (c)) and a reasonable duration for the experiment (5 to 15min, fig. 8 (d)).

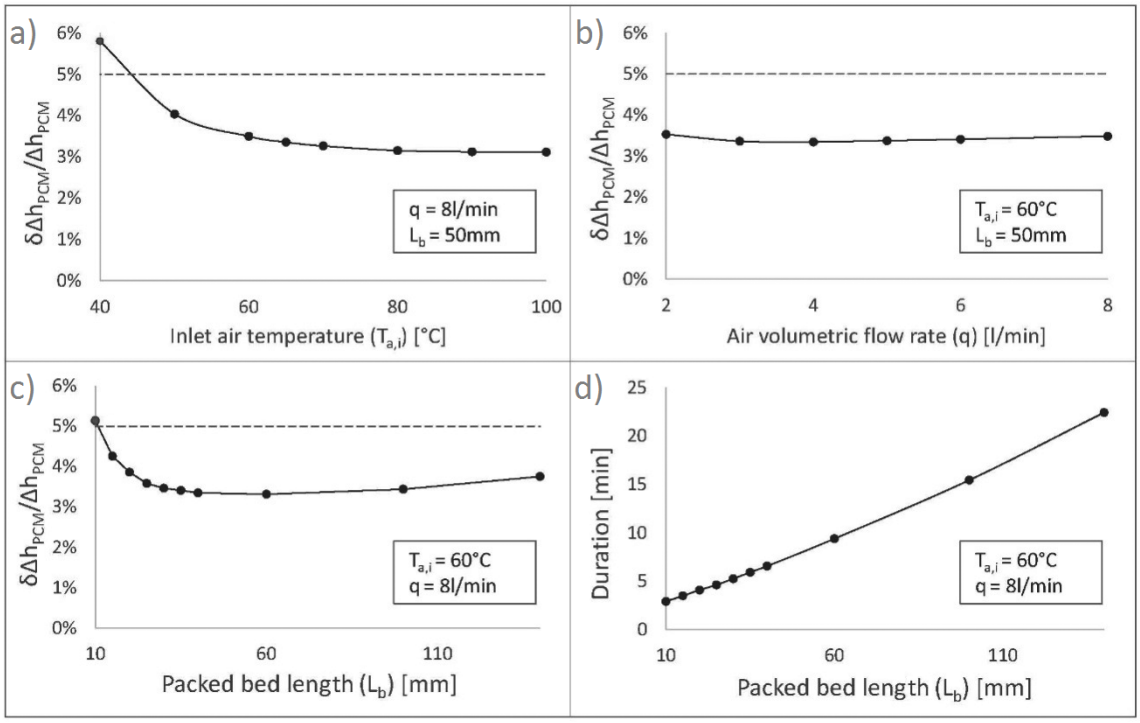

460

461 **Figure 8.** Influence of the experimental conditions (air inlet temperature (a), air volumetric flow
462 rate (b) and packed bed length (c,d)) on the uncertainty propagation of the results and the duration
463 of the experiment.

464 **5.2 Results**

465 Figure 9 shows an example of the temperature evolution of the air and the packed bed container
466 during the test. Table 4 gathers the results from the measurements of GR31. The calculated
467 uncertainty associated with each thermal energy variation is also presented. A good repeatability, less
468 than 5%, has been observed in these experiments.

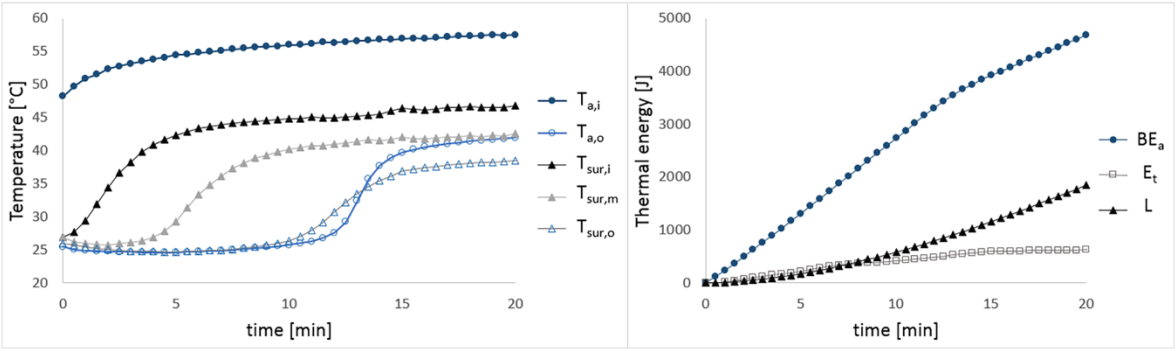

469

470 **Figure 9.** Temperature evolution and thermal energy contributions to the overall energy balance

471 (GR31-T3).

	m_{PCM} [g]	Δh_{PCM} [kJ/kg]	ΔT_{PCM} [°C]	$T_{a,i}$ [°C]	$T_{a-o}\|_{t_\infty}$ [°C]	T_∞ [°C]	$\dot{V}$ [l/min]	$h_{c-r}\|_{t_\infty}$ [W/(m²·K)]
T1	27.65	70.9±3.3	[24.8-46.7]	57.3	41.1	25.5	7.2	14±1
T2	27.63	71.5±3.5	[24.4-48.5]	55.3	40.0	24.5	7.3	13±1
T3	27.65	71.7±3.5	[24.8-49.1]	57.5	43.5	24.7	8	12±1
	Repeatability Δh_{PCM} (σ_{GR31}=1.2kJ/kg)							

472 **Table 4.** Results of the experimental tests (GR31).

473 It should be noted that the measurement model used in this method is based on a simpler hypothesis
474 than that of the T-history method. Whereas in the energy balance methodology the main contribution
475 to the energy variation of the PCM packed bed can be quantified from the thermal energy transferred
476 to the air stream, in the T-history method a uniform temperature inside the samples and an identical
477 equivalent heat transfer coefficient at the surface of both samples (reference and PCM) have to be
478 assumed.

479 Nevertheless, this complementary method is not able to evaluate the enthalpy-temperature curve since
480 the temperature of the packed bed is not uniform during the experiment. Additionally, as discussed
481 in the previous section, the accuracy depends heavily on the experimental conditions. The most
482 relevant variable in the resulting accuracy is the inlet temperature. This effect leads to a lower limit

for the temperature interval in which the enthalpy variation can be measured with acceptable accuracy.

6. Discussion

The results obtained from the application of the different experimental methodologies can be compared in table 5 and figure 10. As can be seen, there is a good agreement between the measured enthalpy variation values. The DSC results obtained with crushed samples are included within the estimated uncertainty range of the T-history and energy balance experimental methods.

Method	c_s [g]	c_l [kJ/kg]	$\overline{T}_m$ [°C]	Δh_{PCM} [kJ/kg] (25-35°C)	Δh_{PCM} [kJ/kg] (24.8-49°C)
DSC granule	1.8±0.3	1.4±0.2	29.4±0.3	64±18	80±21
DSC crushed	1.60±0.05	1.4±0.1	29.9±0.3	54±2	74±5
T-history crushed	1.6±0.4	1.3±0.4	29.0±0.5	52±3	71±4
E. B. set up granule	-	-	-	-	73±4

Table 5. Comparison of the results obtained with the different experimental methodologies.

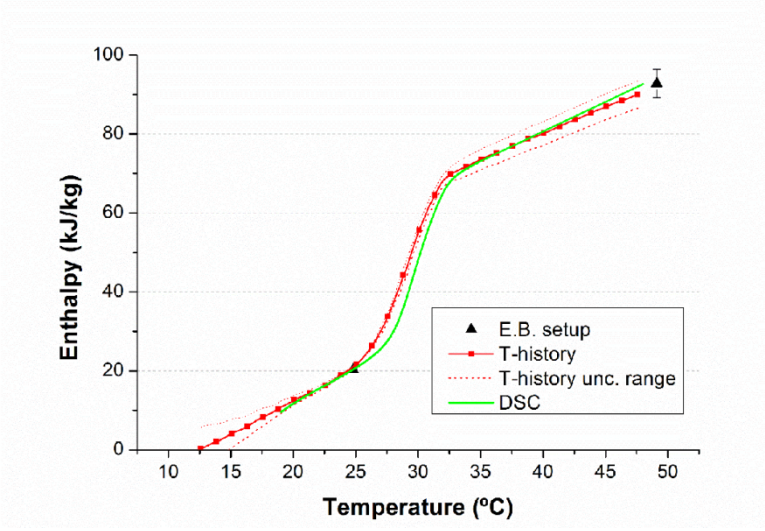

Figure 10. Comparison of the results obtained with the different experimental methodologies.

493 On the other hand, there is an appreciable difference between the phase change temperature of the
494 DSC and T-history measurements (0.9°C). This is not only due to a slight hysteresis phenomenon of
495 the material, but also to a deviation in T-history associated with the thermal gradient inside the PCM
496 sample. According to Mazo et al. [24], the theoretically expected deviation in the measurement of
497 phase change temperature can be bounded by linear functions which are proportional to the Biot
498 number and the temperature difference between the ambient and phase change temperatures (Eq. 14).

499 $$0.44 \cdot Bi_{PCM} \cdot \left|T_\infty - \overline{T}_m\right| \leq \left|\delta T_m\right| \leq 0.70 \cdot Bi_{PCM} \cdot \left|T_\infty - \overline{T}_m\right| \qquad (14)$$

500 The Biot number is conditioned by the experimental configuration and cannot be modified.
501 Furthermore, in the case of crushed samples, it is difficult to estimate the equivalent conductivity and
502 consequently the Biot number. Therefore, if a higher accuracy of the phase change temperature
503 measurement is required, an expansion of the experimental methodology should be developed in
504 order to reduce the effect of this phenomenon. This procedure would involve carrying out thermal
505 tests at reduced ambient temperature differences ($T_\infty - T_m$) in order to reduce the deviation in the
506 phase change temperature measurements associated to the thermal gradients inside the sample. On
507 the other hand, it has to be taken into account that the reduction of this temperature interval ($T_\infty - T_m$)
508 increases the uncertainty of the phase change enthalpy measurement, according to the results of Zhang
509 et al. [23] and Mazo [41].

510 ## 7. Conclusions

511 This work has analyzed some problematic issues associated with the determination of the enthalpy-
512 temperature curves of GPCC by comparing different experimental methodologies. The principal
513 characteristics of these procedures are summarized in the following table (table 6).

514

515

Methodology	h-T curve	Sample mass [g]	Sample form		Advantages	Disadvantages
			Granules	Crushed granules		
DSC	Yes	0.02	Yes	Yes	h-T curve is obtained	If the granule is measured without being crushed, an appropriate sampling must be done. This will lead to a long experiment to get representative results.
					Crushed samples can be measured to reduce the dispersion of the results	The crushed sample preparation can modify phase change temperature
T-history	Yes	8-25	No	Yes	Bigger sample sizes, which means a more representative sample.	Sample must be crushed and compacted to avoid temperature gradients inside the sample. It is difficult to estimate the equivalent conductivity and consequently the Biot number of crushed samples
E.B. setup	No	30	Yes	No	Sample representativeness The model from which the energy variation of PCM is measured is based on a simpler hypothesis than the DSC and T-history methods.	h-T curve cannot be measured. Only the enthalpy variation in a temperature interval. Experimental conditions, especially temperature levels, have a high influence on the accuracy of measurements. Thus, the quality of the measurement limits the temperature interval

Table 6. Main characteristics of experimental methodologies for evaluating enthalpy variations in granular PCM composites.

First of all, the evaluation of the energy balance in the heat exchange between an air stream and a granular PCM packed bed provides a measurement of the enthalpy variation of this composite material. With a suitable design, considerably accurate measurements of the enthalpy variation of representative samples of granular PCM can be obtained. In this case, a repeatable measurement has been obtained that can be used in the comparison with other experimental methodologies.

The results of the DSC analysis have shown a significant deviation in the measurement of the phase change enthalpy variation of three granule samples ($\sigma_{\Delta h}/\Delta h \approx 11\%$). Since these differences can be attributed to the heterogeneity of the composite material, a specific methodology should be developed in order to improve the accuracy of this measurement. Additionally, the equilibrium condition proposed by Lázaro et al. [35] should be verified in each granular PCM composite sample. Therefore, this methodology is very time-consuming.

On the other hand, when crushed samples are used the dispersion in phase change enthalpy measurements is considerably reduced ($\sigma_{\Delta h}/\Delta h \approx 2\%$). Furthermore, these values are consistent with those obtained with the T-history methodology and the energy balance experimental set up. Nevertheless, a slight difference in melting temperature (0.5°C) between the granule sample and the crushed sample was detected. This deviation can be explained in terms of a change of the PCM confinement in the porous material related to the preparation of the crushed sample. Therefore, in a general case, if this sample preparation technique is used, it is recommendable to verify if the resulting modifications of the phase change process are acceptable for a specific application.

Compared to the DSC results, the T-history tests provided a reasonable approximation of the enthalpy-temperature curve. Nevertheless, when the temperature is measured at the surface of the sample, the hysteresis phenomenon is expected to be overestimated [24]. Therefore, it would be of interest to develop a procedure in order to adapt the temperature interval of the T-history test to the required accuracy in phase change temperature measurements.

Acknowledgments

The authors thank the Spanish Ministry of Economy and Competitiveness for the funding of this work within the framework of projects ENE2011-28269-C03-01, ENE2011-22722 and ENE2014- 57262-R, partially funded by the Spanish Government (Energy Program), the Government of Aragon (Spain) and the Social Fund of the European Union (FEDER Program). The authors would like to

547 acknowledge the use of the Servicio General de Apoyo a la Investigación-SAI, Universidad de
548 Zaragoza.

549 **References**

550 [1] K. Nagano, S. Takeda, T. Mochida, K. Shimakura, Thermal characteristics of a direct heat
551 exchange system between granules with phase change material and air, Applied Thermal
552 Engineering 24 (14-15) (2004) 2131-2144.

553 [2] M. Rady, Granular phase change materials for thermal energy storage: Experiments and
554 numerical simulations, Applied Thermal Engineering 29 (14-15) (2009) 3149-3159.

555 [3] M. Rady, Thermal performance of packed bed thermal energy storage units using multiple
556 granular phase change composites, Applied Energy 86 (12) (2009) 2704-2720.

557 [4] M. A. Izquierdo-Barrientos, C. Sobrino, J. A. Almedros-Ibáñez, Thermal energy storage in a
558 fluidized bed of PCM, Chemical Engineering Journal 230 (2013) 573-583.

559 [5] M. A. Izquierdo-Barrientos, M. Fernández-Torrijos, J. A. Almendros-Ibáñez, C. Sobrino,
560 Experimental study of fixed and fluidized beds of PCM with an internal heat exchanger, Applied
561 Thermal Engineering 106 (2016) 1042-1051.

562 [6] K. Nagano, S. Takeda, T. Mochida, K. Shimakura, T. Nakamura, Study of a floor air
563 conditioning phase change material to augment building mass thermal storage. Heat response in
564 small scale experiments, Energy and Buildings 38 (5) (2006) 436-446.

565 [7] D.W. Hawes, Latent Heat Storage in Concrete, (PhD Thesis) Concordia University (1991)
566 Montreal, Quebec (Canada).

567 [8] D. Zhang, Z. Li, J. Zhou, K. Wu, Development of thermal energy storage concrete, Cement and
568 Concrete Research 34 (6) (2004) 927-934.

569 [9] A. R. Sakulich, D. P. Bentz, Incorporation of phase change materials in cementitious systems
570 via fine lightweight aggregate, Construction and Building Materials 35 (2012) 483-490.

571 [10] H. Cui, S. A. Memon, R. Liu, Development, mechanical properties and numerical simulation
572 of macro encapsulated thermal energy storage concrete, Energy and Buildings 96 (2015) 162-174.

573 [11] M. Li, Z. Wu, J. Tan, Heat storage properties of the cement mortar incorporated with
574 composite phase change material, Applied Energy 103 (2013) 393-399.

575 [12] Z. Zhang, G. Shi, S. Wang, X. Fang, X. Liu, Thermal energy storage cement mortar containing
576 n-octadecane/expanded graphite composite phase change material, Renewable Energy 50 (2013)
577 670-675.

578 [13] S. Kim, S. J. Chang, E. Chung, S. G. Jeong, S. Kim, Thermal characteristics of mortar
579 containing hexadecane/xGn SSPCM and energy storage behaviors of envelopes integrated with
580 enhanced heat storage composites for energy efficient buildings, Energy and Buildings 70 (2014)
581 472-479.

582 [14] M. Kheradmand, J. Castro-Gomes, M. Azenha, P. D. Silva, J. L. B. Aguiar, S. E. Zoorob,
583 Assessing the feasibility of impregnating phase change materials in lightweight aggregate for
584 development of thermal energy storage systems, Construction and Building Materials 89 (2015) 48-
585 59.

586 [15] N. P. Sharifi, A. Sakulich, Application of phase change materials to improve the thermal
587 performance of cementitious material, Energy and Buildings 103 (2015) 83-85.

588 [16] M. A. Izquierdo-Barrientos, C. Sobrino, J. A. Almedros-Ibáñez, C. Barreneche, N. Ellis, L. F.
589 Cabeza, Characterization of granular phase change materials for thermal energy storage applications
590 in fluidized beds, Applied Energy 181 (2016) 310-321.

591 [17] M. Rady, Study of phase changing characteristics of granular composites using differential
592 scanning calorimetry, Energy Conversion and Management 50 (5) (2009) 1210-1217.

593 [18] M. Rady, E. Arquis, A comparative study of phase changing characteristics of granular phase
594 change materials using DSC and T-history methods, Fluid Dynamics & Materials Processing 6 (2)
595 (2010) 137-152.

596 [19] D. Zhang, J. Zhou, K. Wu, Z. Li, Granular phase changing composites for thermal energy
597 storage, Solar Energy 78 (3) (2005) 471-480.

598 [20] D. Zhang, S. Tian, D. Xiao, Experimental study on the phase change behavior of phase change
599 material confined in pores, Solar Energy 81 (5) (2007) 653-660.

600 [21] X. Li, J. G. Sanjayan, J. L. Wilson, Fabrication and stability of form-stable diatomite/paraffin
601 phase change material composites, Energy and Buildings 76 (2014) 284-294.

602 [22] X. Li, H. Chen, L. Liu, Z. Lu, J. G. Sanjayan, W. H. Duan, Development of granular expanded
603 perlite/paraffin phase change material composites and prevention of leakage, Solar Energy 137
604 (2016) 179-188.

605 [23] Y. Zhang, Y. Jiang, Y. Jiang, A simple method, the T-history method, of determining the heat
606 of fusion, specific heat and thermal conductivity of phase-change materials, Measurement Science
607 and Technology 10 (1999) 201-205.

608 [24] J. Mazo, M. Delgado, A. Lázaro, P. Dolado, C. Peñalosa, J.M. Marín, B. Zalba, A theoretical
609 study on the accuracy of the T-history method for enthalpy-temperature curve measurement:
610 analysis of the influence of thermal gradients inside T-history samples, Measurement Science and
611 Technology 26 (12) (2015) 125001.

612 [25] M. A. Rady, E. Arquis, C. Le Bot, Characterization of granular phase changing composites for
613 energy storage using the T-history method, International Journal of Energy Research 34 (4) (2010)
614 333-344.

615 [26] RUBITHERM GmbH, www.rubitherm.de, (accessed 8.3.17)

616 [27] J. M. Marín, B. Zalba, L. F. Cabeza, H. Mehling, Determination of enthalpy-temperature
617 curves of phase change materials with the temperature-history method: improvement to temperature
618 dependent properties, Measurements Science and Technology 14 (2003) 184-189.

619 [28] B. Zalba, J.M. Marín, L.F. Cabeza, H. Mehling, Free-cooling of buildings with phase change
620 materials, International Journal of Refrigeration 27 (8) (2004) 839-849.

621 [29] E. Günther, S. Hiebler, H. Mehling, Determination of the heat storage capacity of PCM and
622 PCM-objects as a function of temperature, Proceedings of ECOSTOCK, Stockton (USA) (2006).

623 [30] H.K. Christenson, Confinement effects on freezing and melting, Journal of Physics: Condensed
624 Matter 13 (2001) 95-133.

625 [31] D. Zhang, K. Wu, Z. Li, Tuning effect of porous media's structure on the phase changing
626 behavior of organic phase changing matters, Journal of Tongji University 32 (2014) 1163-1167.

627 [32] Z. Fu, L. Su, M. Liu, J. Li, Z. Zhang, B. Li, Confinement effect of silica mesopores on thermal
628 behaviour of phase change materials, Journal of Sol-Gel Science Technology 50 (2016) 180-188.

629 [33] E. Günther, S. Hiebler, H. Mehling, R. Redlich, Enthalpy of phase change materials as a function
630 of temperature: required accuracy and suitable measurement methods, International Journal of
631 Thermophysics 30 (2009) 1257-1269.

632 [34] M.S. Toas, D.G. Ober, M.P. Ellis, Loose fill insulation product having phase change material
633 therein (2006) EP1628110A1.

[35] A. Lazaro, C. Peñalosa, A. Solé, G. Diarce, T. Haussmann, M. Fois, B. Zalba, S. Gschwander, L.F. Cabeza, Intercomparative tests on phase change materials characterization with differential scanning calorimeter, Applied Energy 109 (2013) 415-420.

[36] ASTM E1269—11 Standard test method for determining specific heat capacity by differential scanning calorimetry, ASTM International.

[37] BIPM, IEC, IFCC, ISO, IUPAC, IUPAP, OIML, Evaluation of measurement data. Guide to the expansion of uncertainty in measurement JCGM 100: 2008, 1st edition, Sèvres (2008) BIPM Joint Committee for Guides in Metrology.

[38] S. Rudtsch, Uncertainty of heat capacity measurements with differential scanning calorimeters, Termochimica Acta, 382 (2002) 17-25.

[39] B. Wilthan, Uncertainty budget for high temperature heat flux DSCs, Journal of Thermal Analysis and Calorimetry, 118 (2014) 603-611.

[40] S. M. Sarge, G. W. H. Höhne, W. Hemminger, Calorimetry. Fundamentals, instrumentation and applications, Wiley-WCH, Weinheim, Germany, 2014.

[41] J. Mazo, Research about the application of thermal energy storage with PCM in thermally activated building elements, Ph.D. Thesis (2016) Zaragoza.

[42] E. Palomo del Barrio, J. L. Dauvergne, A non-parametric method for estimating enthalpy-temperature functions of shape-stabilized phase material, International Journal of Heat and Mass Transfer 54 (2011) 1268-1277.

[43] A. Lázaro, Thermal Energy Storage with Phase Change Materials. Building applications: Material behavior characterization and experimental setup for testing air-PCM heat exchangers, Ph.D. Thesis (2008) Universidad de Zaragoza.

656 [44] H. Hong, C. Kang, J.H. Peck, Measurement methods of latent heat for PCM with low melting
657 temperature in closed tube, International Journal of Air-Conditioning and Refrigeration 12 (4)
658 (2004) 206-213.

659 [45] H. Hong, S.K. Kim, Y.S. Kim, Accuracy improvement of T-history method for measuring heat
660 of fusion of various materials, International Journal of Refrigeration 27 (4) (2004) 360-366.

661 [46] P. Dolado, I. Miranda, J.S. Urieta, J. Coronas, A. Lázaro, Packed bed zeolite experimental
662 setup to study TCS systems up to 200ºC, Eurosun 2014 (2014), Aix-les Bains, France.

663 [47] Bronkhorst, http://www.bronkhorst.com/files/downloads/brochures/folder-el-flow.pdf,
664 (accessed 8.3.17)

665 [48] F. P. Incropera, D. P. DeWitt, T. L. Bergman, A. S. Lavine, Fundamentals of heat and mass
666 transfer, United States of America (2007) John Wiley & Sons.

667 [49] S.W. Churchill, H.H.S. Chu, Correlating equations for laminar and turbulent free convection
668 from a horizontal cylinder, International Journal of Heat and Mass Transfer 18 (9) (1975) 1049-
669 1053.

670 [50] M. A. Izquierdo-Barrientos, Heat transfer and thermal storage in fixed and fluidized beds of
671 phase change material, PhD Thesis (2014) University of Carlos III, Madrid (Spain).

672 [51] M. A. Izquierdo-Barrientos, C. Sobrino, J. A. Almedros-Ibáñez, Modeling and experiments of
673 energy storage in a packed bed with PCM, International Journal of Multiphase Flow 86 (2016) 1-9.

674 [52] N. Wakao, S. Kaguei, T. Funazkri, Effect of fluid dispersion coefficients on particle to fluid
675 heat transfer coefficients in packed beds, Chemical Engineering Science 34 (3) (1979) 325-336.

676 [53] S. V. Patankar, Numerical heat transfer and fluid flow, New York (1980) McGraw-Hill.